

Full-scale tests of skirt penetration resistance in gravel for offshore wind structures

Varela, Elena ; Miranda, Marina ; Castro, Jorge ; Sarmiento, Javier ; Guanche, Raúl

Author affiliations:

Elena Varela, varelae@unican.es, Group of Geotechnical Engineering. Department of Ground Engineering and Materials Science, Universidad de Cantabria, ETSI Caminos, Canales y Puertos. Avda. de los Castros s/n. 39005. Santander, Spain

Marina Miranda, mirandama@unican.es, Group of Geotechnical Engineering. Department of Ground Engineering and Materials Science, Universidad de Cantabria, ETSI Caminos, Canales y Puertos. Avda. de los Castros s/n. 39005. Santander, Spain

Jorge Castro, corresponding author, castrogj@unican.es, Group of Geotech. Eng. Department of Ground Eng. and Materials Science, Universidad de Cantabria, ETSI Caminos, Canales y Puertos. Avda. de los Castros s/n. 39005. Santander, Spain

Javier Sarmiento, sarmientoj@unican.es, IHCantabria - Instituto de Hidráulica Ambiental de la Universidad de Cantabria. Isabel Torres 15, PCTCAN. Santander, Spain

Raúl Guanche, guancher@unican.es, IHCantabria - Instituto de Hidráulica Ambiental de la Universidad de Cantabria. Isabel Torres 15, PCTCAN. Santander, Spain

ABSTRACT

Full-scale tests were performed to study the penetration resistance of steel plates (skirts), which are common foundation elements of jacket offshore wind structures. Penetration resistance is well studied in clays and sands, but there is limited information on penetration in gravels, which are typically used as the scour protection of critical elements like offshore wind substations. Direct extrapolation of penetration resistance in sands is not possible because of the grain size effect. Two steel plate thicknesses and two gravel sizes were used to study the influence of the grain size effect on the penetration resistance. Moreover, the importance of tip shape has also been evaluated by means of bevelled tip tests. The results of the experimental tests show a strong dependence of penetration resistance on penetration depth as expected, but also a significative dependence on skirt thickness and gravel grain size. A good agreement with experimental results has been found when analytically interpreting the penetration resistance using traditional bearing capacity formulae, but with an equivalent skirt thickness equal to the real skirt thickness plus the mean grain size, to account for the grain size effect.

KEYWORDS: Offshore, Foundations, Full-scale test, Gravel, Skirt, Penetration.

NOTATION

A_{tip}	Skirt tip area
A_{side}	Skirt side area
d_{50}	Mean grain size
f_s	Side wall friction
K	Coefficient of lateral earth pressure
N_q, N_γ	Bearing capacity factors
q	Effective overburden pressure at the tip level
q_{tip}	Skirt tip resistance per square meter
R	Penetration resistance
R_{tip}	Skirt tip resistance
R_{side}	Skirt wall resistance
t	Skirt thickness
t_{eq}	Equivalent skirt thickness
z	Vertical displacement
ϕ	Friction angle
γ'	Effective (submerged) unit weight
δ	Interface friction angle between skirt and soil

1 INTRODUCTION

The increasing demand for renewable energy has resulted in the use of the oceans as an important source of wind and marine renewable energies and the development of large offshore wind farms and structures. The foundation of offshore wind structures, and in particular critical structures like Offshore Substations (OSS), poses new challenges to offshore geotechnics. In many cases, such as in skirted or mud-mat foundations, penetration of steel elements into the sea bottom is required to ensure structure stability. Existing standards and recommended best practices provide guidance in evaluating the penetration resistance of these steel elements into cohesive or sandy soils, but limited information exists about penetration resistance in gravels, which are the base of scour protections. This paper addresses this scientific gap accounting for the influence of the gravel grain size through full-scale tests (Figure 1).

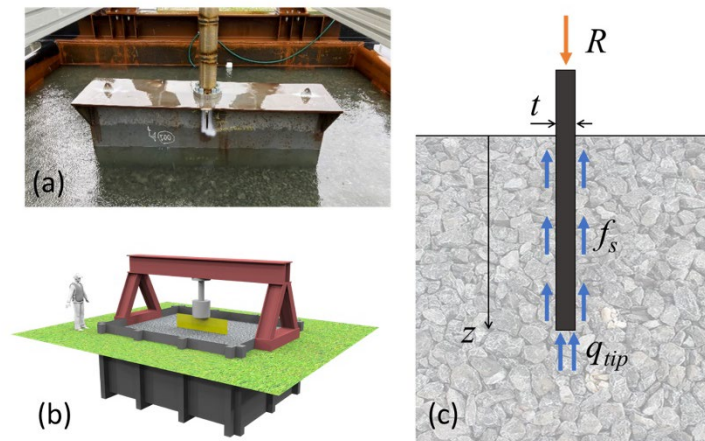


Figure 1. Penetration resistance of a steel plate in gravel: (a) Full-scale test; (b) Conceptualization of full-scale tests; (c) Cross section for theoretical analyses (R includes the plate self-weight).

This research is motivated by the design of the jacket foundation for the DolWin kappa OSS, within the framework of DolWin6 project (Wadden Sea, Germany), a 900-megawatt DC connection promoted by TenneT. The jacket solution selected is a post-piled structure, which requires a scour protection system to ensure the stability of the structure due to potential flow amplification around it and the potential triggering of sediment mobility processes. Scour protection systems are typically composed of a combination of armour layer and filter layer (e.g., Sonnevile et al. 2014; Escribano and Brennan 2017) and they are installed in advance for safety reasons (impact reduction over the jacket primary and secondary steel structure elements).

The post-pile jacket structure needs to ensure sufficient stability against the action of environmental loads (essentially wind, waves and currents) between the jacket deployment and the piling. The stability during this interim is ensured by means of the introduction of steel plates (flat bars or skirts) in the mud mat of the jacket. This helps to increase the sliding bearing capacity ensuring the integrity of the structure.

The installation of the OSS jacket is made directly over the scour protection, formed by high density eclogite gravel. Therefore, the penetration of the steel plates, included on the footprint of the OSS jacket, must be ensured thanks to its own self-weight during installation and an accurate estimation of the penetration resistance is vital for a successful installation process.

The analysis of the penetration resistance of steel plates is also required in related problems, such as gravity-based foundations with shear keys, mud-mats or skirted foundations (e.g., Mana et al. 2013; Feng et al. 2014; Martin et al. 2015; Bienen et al. 2012), and is needed for a correct installation of the structure (e.g., Senders and Randolph 2009; Villalobos et al. 2010; Lian et al. 2014; Liu et al. 2019).

Some standards or recommended best practices, namely API RP 2GEO (2011) and DNVGL (2017), provide guidance in evaluating the penetration resistance, by means of bearing capacity formulae or correlations with cone penetration resistances, respectively. Also, some authors (e.g., Andersen et al. 2008; Houlsby and Byrne 2005) have further studied the penetration resistance of skirted elements. However, all these studies are focused either on cohesive soils or on sandy soils (fine-grained, non-cohesive soils). Hence, there is limited experience and information in the literature about penetration resistance in gravels.

As presented in the paper, direct extrapolation of formulations for sandy soils to gravels, by adjusting the frictional properties, is not possible due to the influence of the gravel grain size. When the mean grain size (d_{50}) starts to be comparable to the steel plate thickness (t), it notably influences the penetration resistance. Bolton et al. (1999) studied this particle size effect for cone penetration testing (CPT) in sands and found that some extra resistance is anticipated when the ratio between the cone diameter and the mean grain size falls below about 20. Arroyo et al. (2011) and Li and Wu (2012) found a similar particle size effect (including noise, i.e., oscillations, in the results) using discrete element models and varying the diameter of the cone. More recently, Miyai et al. (2019) presented

a notable contribution on the influence of the particle size on plate penetration. However, Miyai et al. (2019) is based on numerical simulations with t/d_{50} values between 2.6 and 63. For gravels, t/d_{50} is lower and it could be in an approximate range between 0.2 and 20.

In order to fill the above-mentioned gap concerning skirt penetration resistance in gravel, full-scale tests were performed (Figure 1). Two gravel sizes and different steel plate thicknesses, with t/d_{50} ratios in the range between 0.3 and 1.6, were used to extend the current knowledge. Moreover, the shape of the plate tip was also investigated, using steel plates with a flat tip and a bevelled tip, as bevelling or tamping the tip of the skirts reduces the penetration resistance (e.g., Wu et al. 2021). Only plane (i.e., without curvature) and single elements are considered. The effect of skirt curvature on its own is expected to be minor, but the interaction between penetrating elements plays a role as studied, for example, by Houlsby and Byrne (2005) or Mana et al. (2013). This interaction effect may increase the penetration resistance, but it is beyond the scope of this paper.

The present paper is organized as follows: the test methodology is described in Section 2, which outlines the testing procedure, as well as the main properties of the gravel, the skirts and the instrumentation strategy. Next, the results in terms of penetration resistance are presented in Section 3 and Section 4 summarizes the semi-empirical approach directly derived from the experimental results. Finally, some conclusions are drawn (Section 5).

2 TEST SETUP

On-site testing is always the preferred option when discussing geotechnical issues. However, field testing traditionally shows technical and cost barriers that prevent the development of comprehensive test programs. The proposed experimental program attempts to overcome the potential testing uncertainties. It was designed to narrow down potential uncertainties derived from the scale effects by means of a real scale test (1/1 scale) program. A test bench has been specifically designed, manufactured and installed at IHCantabria facilities in Santander (see Figure 2), which provided the necessary space, access, and monitoring equipment. The following sub-sections describe the test setup in detail, from the equipment, material and tested skirts to the procedure and measuring system.



Figure 2. Testing site.

2.1 Test bench

A dedicated container has been designed to ensure a watertight environment, to minimize the required volume of gravel and to facilitate the allocation of a 1000 kN jack. The container is made of steel, and its external dimensions are: 5 x 5 x 2.5 m. It has horizontal and vertical stiffeners to prevent structural deformation during the testing process. The total volume of the container is 59.54 m³. To facilitate the operativity of the test bench, the container was buried in the ground, so that the top part of the container was approximately at the ground surface level. A loading frame was rigidly connected to the container by means of a bolted connection. The loading frame was structurally designed to support the necessary applied vertical forces, up to 1000 kN in the center thanks to a hydraulic jack. Finally, an auxiliary crane has been installed in order to ease the maneuvering of loads (see Figure 2).

2.2 Gravel material

The scour protection design for DolWin kappa required a high-density gravel. From all the potential alternatives, eclogite gravel from Norway was chosen. In order to reduce

potential uncertainties, this gravel has been shipped and used for testing. Its main properties are given in Table 1.

Table 1. Some physical properties of the eclogite gravel.

Unit weight of solid particles (kN/m ³)	32	
Angle of repose	34°	
	Loose	Compacted
Dry Bulk Unit Weight (kN/m ³)	17	18.5
Expected Saturated Unit Weight (kN/m ³)	22	23
Expected Submerged Unit Weight (kN/m ³)	12	12.6

Two grain size distributions have been used. The first one was a 0.5-1.5" gravel, with a mean grain size (d_{50}) of around 1" (25 mm), and the second one was a 1-3" gravel, with a d_{50} of 2" (50 mm). Several granulometric (sieving) analyses were performed on each type of eclogite gravel to obtain the grain size distribution curves. The samples were directly and randomly obtained from the supplied eclogite. Figure 3 shows the results of the sieving analyses performed for the 0.5"-1.5" gravel and Figure 3 for the 1"-3" gravel. From them, it can be concluded that the material showed a good homogeneity since the grain size distribution curves indicate a good agreement between them. Moreover, in Figure 4, the dashed-lined curve represents the grain size distribution of the gravel after a penetration test with a non-beveled skirt. The sieving analysis after a penetration test was performed to evaluate particle breakage during the tests. The results seem to indicate that despite some occasional grain breakages that were observed during and after testing, the grain size distribution curves of the gravels did not change perceptibly. Therefore, particle breakage shows a limited rate that cannot be perceived by the sieving curve.

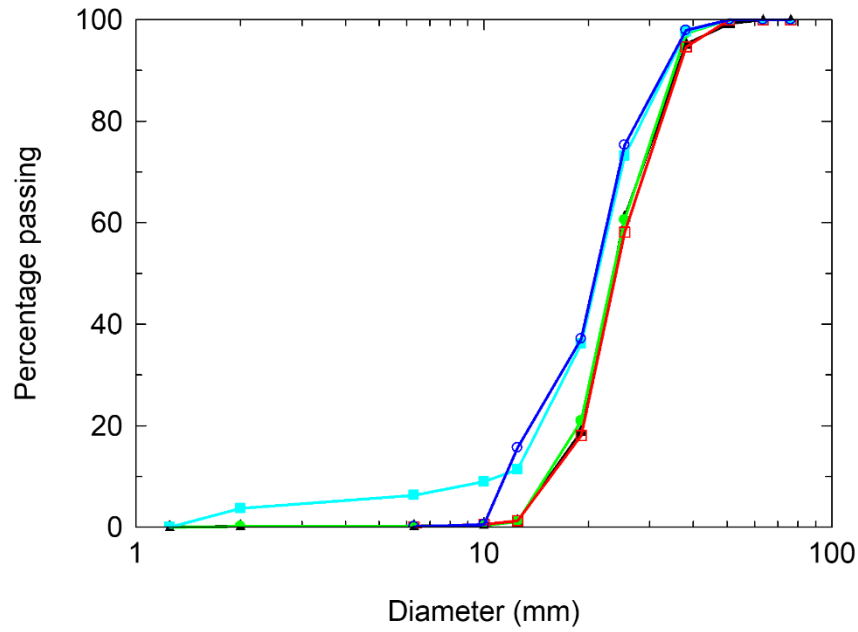


Figure 3. Grain size distribution tests performed on the 0.5''-1.5'' eclogite.

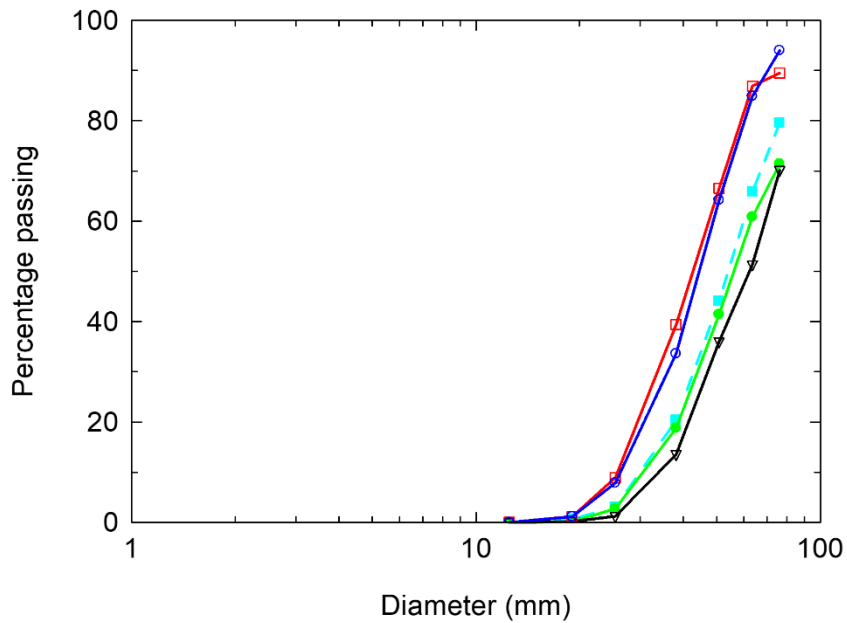


Figure 4. Grain size distribution tests performed on the 1''-3'' eclogite (dashed line: after a penetration test).

The deployment of the gravel on the seabed influences its unit weight and, although the variation in the gravel unit weight with the degree of compaction is limited (Table 1) because the gravel is uniform (Figure 3 and Figure 4), it has an impact on the gravel friction, and consequently, on the penetration resistance. To ensure the maximum levels

of fidelity, a specific study was performed to define the filling process to replicate the “in situ” deployment conditions by means of a controlled granular material placement strategy.

A gravel particle of eclogite of 50 mm of diameter free falling in sea water reaches its terminal velocity in calm water at 1.7 m/s and for a falling height of more than 0.5 m (e.g., Riazi and Türker 2019). During scour protection placement, the gravel will be free falling in sea water more than the threshold falling height, namely 0.5 m, reaching the seabed at approximately the terminal velocity. On the other hand, during the experimental tests, it may be dropped directly from the air and the differences between the resistance in air and water must be considered. This equivalent distance is around 150 mm (see Figure 5). Therefore, the free fall distance should be kept around 100-200 mm in air or longer than 500 mm under water during the pouring of the gravel into the test tank. A similar analysis was performed for the smaller gravel ($d_{50} = 25$ mm), when terminal velocity in water is reached at 400 mm free falling and around 75 mm free falling in the air.

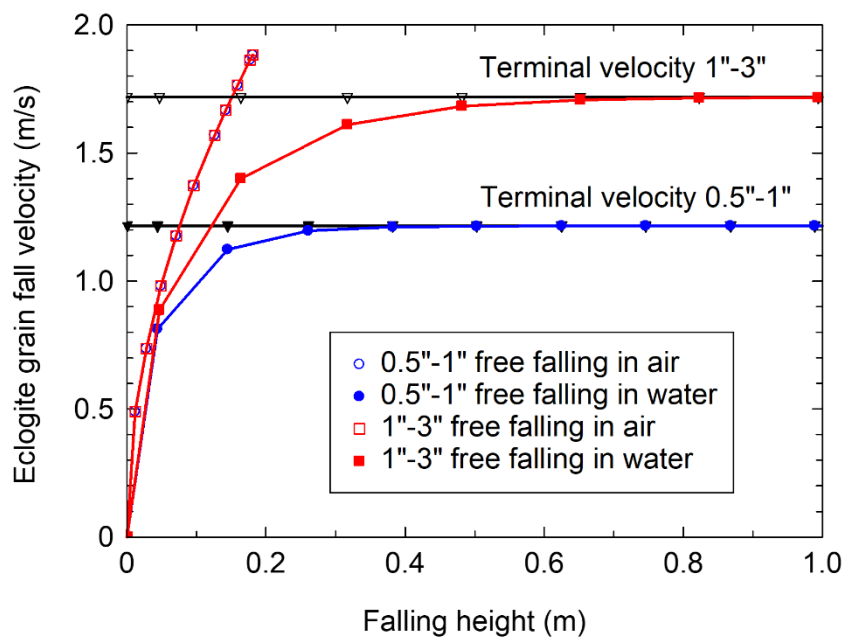


Figure 5. Pouring analysis of a 50 mm and a 25mm diameter grain eclogite particle.

The test setup procedure followed ensured that the gravel was poured from 500 mm height under water. This was applied to the initial layers. The next layers were poured from 100

mm in the air. This procedure provided a dry bulk density of 1,730 kg/m³ in the case of the 0.5”-1.5” gravel. In the case of the 1”-3” gravel, the dry bulk density obtained was 1,770 kg/m³. Both densities were within the range provided by the supplier (Table 1). This range is just approximate and does not consider a specific grain size distribution. Consequently, it should not be used to calculate relative densities.

2.3 Skirts setup

Two steel skirt thicknesses were tested, namely 15 mm and 80 mm. Moreover, to analyze how the shape of the skirt tip may influence the penetration resistance, two 15 mm-thick skirts were tested, one with a flat tip and another with a bevelled tip with a width of 5 mm. The 80 mm-thick skirt had a flat tip. Consequently, three different skirts were used in the test program (see Figure 6 and Figure 7). The ratio between those skirt thicknesses (t) and the d_{50} of the gravels is between 0.3 and 3.2. The steel plates (skirts) were plane. The free height of the 15 mm-thick skirts allowed for up to 700 mm of penetration, while the 80 mm-thick skirt allowed for 950 mm of penetration (see Figure 7). The length of the 15 mm-thick skirts was 2 meters. This length was reduced down to 1 meter for the 80 mm-thick skirt to reduce the required penetrating force (hydraulic jack limitations).

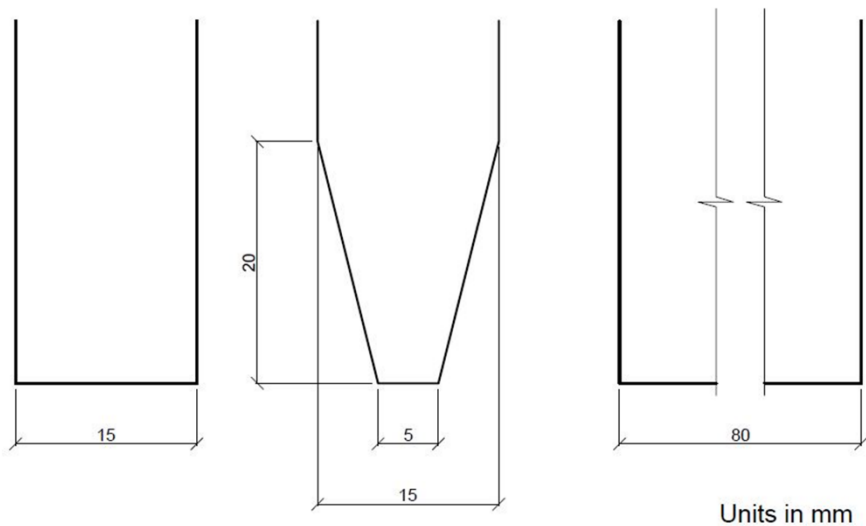


Figure 6. Dimensions of the three tested skirts.

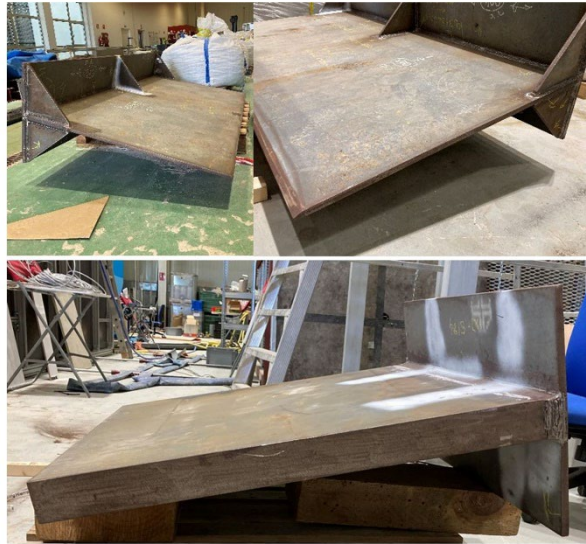


Figure 7. Pictures of the three different skirts tested. On the top left, 15 mm-thick flat tip, on the top right, 15 mm-thick bevelled tip and on the bottom, 80 mm-thick flat tip.

2.4 Test program and instrumentation strategy

A total of 22 tests were carried out with both gravels and the different skirts. The repetitiveness of the tests was ensured through 4 per test. The maximum penetration depth was about 300 mm, but in some cases an additional test was performed or the target skirt penetration depth was greater to improve the interpretation of results. The value of the maximum penetration depth was limited by the load cell capacity. A summary of the tests performed can be seen in Table 2.

Table 2. Test repetitions for the different test configurations: skirt thickness, gravel particle size and maximum penetration depth.

	$t = 15\text{mm}$	$t = 15\text{mm bevelled}$	$t = 80\text{mm}$
$d_{50}=25\text{ mm}$	4 ($z < 350\text{ mm}$)	4 ($z < 400\text{ mm}$)	0
$d_{50}=50\text{ mm}$	4 ($z < 300\text{ mm}$) 1 ($z < 500\text{ mm}$)	5 ($z < 300\text{ mm}$)	4 ($z < 950\text{ mm}$)

The test procedure was identical for all the configurations. Once the material was in place, each skirt was pushed (jacked) into the granular material by means of a hydraulic jack supported by the metal frame above the container (see Figure 8).

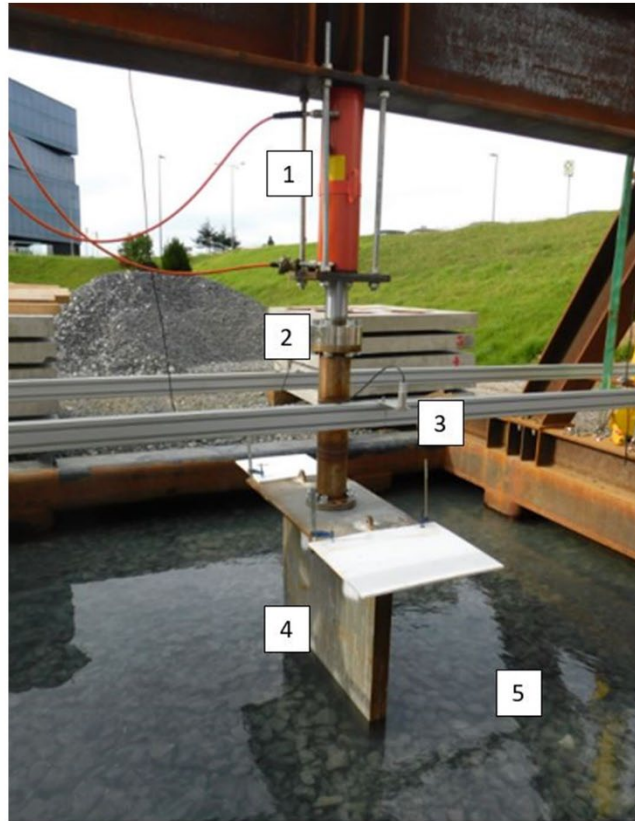


Figure 8. Test setup: (1) Hydraulic jack; (2) Load cell; (3) Displacement sensor; (4) Skirt; (5) Eclogite gravel.



Figure 9. Scratches observed near the tip of the skirts after testing in 1''-3'' gravel.

Both vertical displacement and vertical load were measured during each test. The displacement of the skirt was recorded using two ultrasonic displacement sensors (see Figure 8, #3). Having two sensors enables the control of the penetration and of the tilting of the skirts. Thanks to a load cell, located next to the hydraulic jack, the penetration resistance was measured. Two different load cells were employed depending

on the expected penetration resistance, namely one with a capacity of 100 kN for the tests performed with the 15 mm-thick skirts, and an alternative load cell with a capacity of 1,000 kN for the tests with the 80 mm-thick skirt. The hydraulic jack has a maximum capacity of 1,000 kN and a maximum stroke of 500 mm. Thus, for tests with the 80 mm-thick skirt, which had a target maximum penetration depth of 950 mm, the test procedure was a step-based one combining the available stroke with coupling steel extensions to the hydraulic jack. After two iterations, the target depth was achieved. It should be noted that this procedure implies a loading-unloading-reloading cycle at a penetration depth of around 500 mm. From the results obtained, it can be concluded that this procedure has no noticeable influence on the results, as shown in the next section. In all cases, the skirts were bolted to the hydraulic jack and the load cell; therefore, their own weight was supported by the frame (see Figure 8) and the recorded load was only that applied with the hydraulic jack. At the end of each test, after taking out the skirt, the gravel affected by the skirt penetration was replaced by new gravel leaving the layer with a similar density for each test. The skirts and their tips were not damaged during the tests and only minor scratches were visible. Thus, replacement of the skirts was not necessary (see Figure 9).

3 EXPERIMENTAL RESULTS

3.1 Flat tip skirts

3.1.1 15 mm-thick skirt

The experimental results in terms of penetration resistance versus penetration depth and their linear fittings for the 15 mm-thick flat tip skirt in both gravels are presented in Figure 10. As expected, the load required to jack the skirt through the gravel with the larger grain size is higher. Besides, the penetration resistance notably oscillates (noise), which is mainly a consequence of the grain size effect as found, for instance, by Arroyo et al. (2011), Lin and Wu (2012) and Miyai et al. (2019). The larger the gravel is, the higher the oscillations recorded. Therefore, they are more noticeable for the larger gravel grain size (1"-3"), for which the t/d_{50} ratio is 0.3, than for the 0.5-1.5" gravel with a t/d_{50} ratio of 0.6.

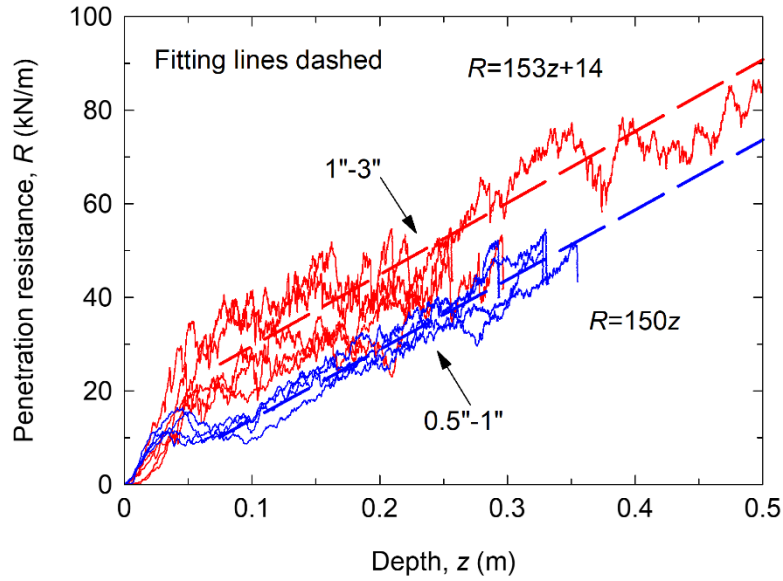


Figure 10. Penetration resistance of 15 mm-thick flat tip skirt in both gravels.

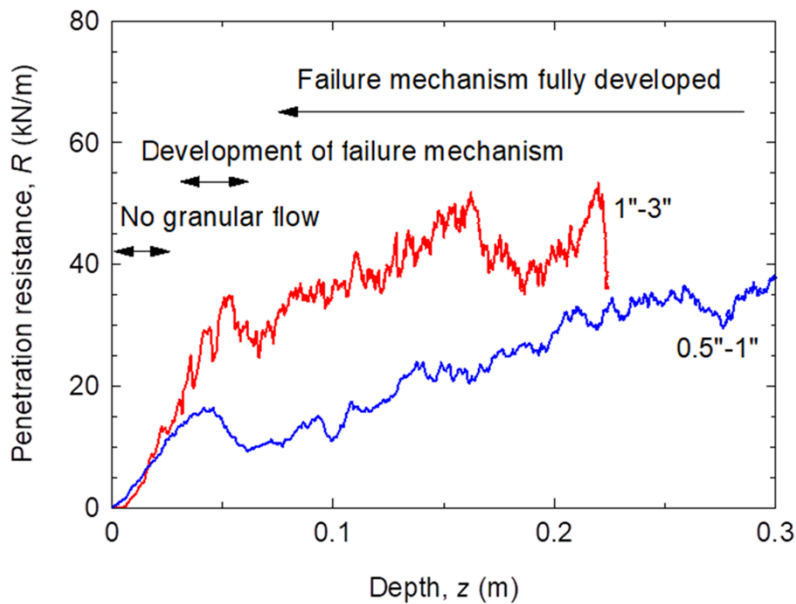


Figure 11. Visualization of the skirt penetration phases (15-mm thick flat tip skirt).

The increase in the penetration resistance with the vertical displacement (penetration depth) follows the same trend for both gravels and three different phases may be distinguished (Figure 11): (1) an initial part with no granular flow (elasto-plastic behavior prior to failure), where the load increases heavily with the displacement (approximately up to 0.05 m) and only minor oscillations (associated with the granular flow) are observed; (2) an intermediate or transient phase, where the load-displacement curves

show a decrease and a plateau, associated with the triggering of the penetration mechanism (soil failure and flow of gravel grains); (3) a final phase, where the penetration mechanism (granular flow) is completely developed and the penetration resistance increases linearly with the penetration depth. The slope of the load-displacement curves for this final phase appears to be almost identical for both gravels, which is not a theoretically expected result and is attributed to the oscillations and variability of the field measurements. On the other hand, the slope of the initial part shows significant differences between them. The 1-3" gravel shows a higher threshold until the penetration mechanism is fully developed, almost three times higher than the 0.5-1.5" gravel. The linear fittings (dashed lines in Figure 10) have been obtained for penetration depths above 0.075 m because from that point the penetration mechanism seems to be fully developed (phase 3).

The theoretical background for the linear fittings is that the penetration resistance has two main components: (a) the tip resistance and (b) the side wall (shaft) resistance (e.g., Andersen et al. 2008) (Figure 1). In this case, the contribution of the shaft resistance, which increases with the square of the penetration depth here, is limited in comparison with the tip resistance, which varies linearly with the penetration depth. The tip resistance is clearly the major component of the penetration resistance for the present cases, around 98%, as will be theoretically derived in the next section. From this theoretical point of view, both linear fittings should have an intercept that could be interpreted as the tip resistance for $z=0$. The null value for the 0.5-1.5" gravel may be attributed to the oscillations and variability of the field measurements and the non-conditioned fitting process. This null intercept also results in a higher than expected slope as mentioned above.

3.1.2 80 mm-thick skirt

Figure 12 summarizes the experimental results and linear fitting of the 80 mm-thick non-bevelled skirt in the 1"-3" gravel ($d_{50}=50\text{mm}$). As already mentioned, the unloading-reloading loops for a depth of around 0.5 m were necessary for the readjustment of the hydraulic jack, since its displacement range was not enough to perform the test in one go. These unloading-reloading cycles have a negligible influence on the load-displacement curves (Figure 12). Besides, they are nearly vertical, showing that the elastic part of the

vertical displacement is negligible. On the other hand, the increase in the vertical load with the penetration depth follows the same trend as in the case of the 15 mm-thick skirts. The initial part where the load increases sharply with the penetration depth associated with the development of the penetration mechanism took place until an approximate depth of 0.075 m. Then, once the penetration mechanism had been fully developed, a constant slope penetration resistance law was measured and fitted to a straight line.

Comparing the penetration resistances of the 15 mm-thick and 80-mm thick skirts in the 1"-3" gravel, the influence of skirt thickness and the grain size effect can be analysed. As expected, the penetration resistance (R) is higher for the thicker plate, 2 times greater at a depth of $z=0.1$ m (29 kN/m vs. 59 kN/m) and 2.5 times at a depth of $z=0.35$ m (68 vs. 171 kN/m). In contrast, the penetration pressure (mainly tip pressure) is higher for the thinner plate; for instance, for $z=0.1$ m, the penetration pressure is 2.0 MPa for $t=15$ mm and 0.7 MPa for $t=80$ mm (nearly 3 times higher), while for $z=0.35$ m, the penetration pressure is 4.5 MPa for $t=15$ mm and 2.1 MPa for $t=80$ mm (more than 2 times higher). As detailed in the next section, a higher pressure for the thinner plate cannot be justified using traditional bearing capacity formulae; it is explained because the thinner plate has a more notable grain size effect (the value of the t/d_{50} ratios are 0.3 and 1.6 for the cases of 15 mm- and 80 mm-thick skirts, respectively). Besides, from the values of the penetration pressures above, it is observed that the increase in the penetration pressure due to the grain size effect reduces with the penetration depth.

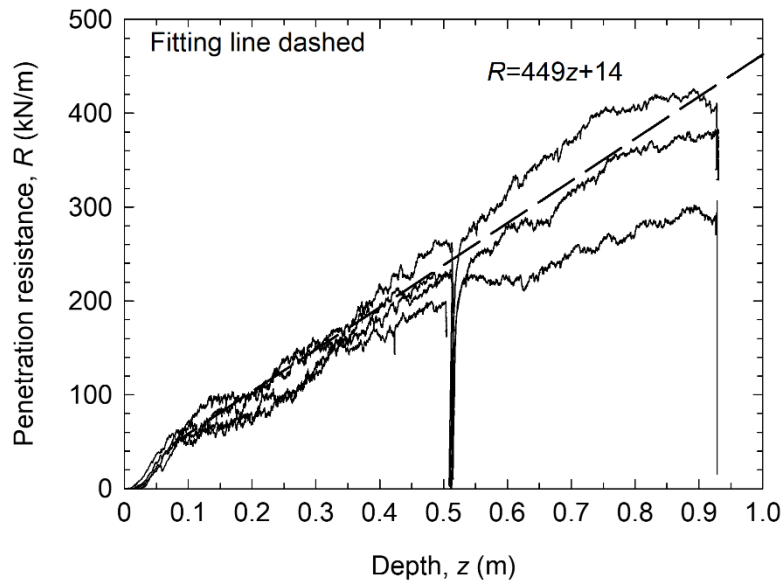


Figure 12. Penetration resistance of 80 mm-thick flat tip skirt in 1"-3" gravel.

3.2 Bevelled skirts

To study the influence of the tip shape, a 15 mm-thick bevelled skirt (see Figure 6) was tested in both gravels. Figure 13 shows the results of the experimental tests and the linear fittings for both gravel sizes.

In keeping with previous results, a higher load is required to jack the skirt into the 1"-3" gravel and the oscillations and the initial increase in the penetration resistance are larger for the 1"-3" gravel ($d_{50}=50\text{mm}$). Comparing the results with those of the 15 mm-thick flat tip skirt (see Figure 10), the bevelled skirt requires less vertical load to be jacked into both gravels, as expected. However, the differences are small in both cases (less than 10%). The differences are slightly higher in the case of the finer gravel ($d_{50}=25\text{mm}$) (see Table 3). The greater reduction in the finer gravel may be attributed to the grain size effect, i.e., the influence of bevelling the skirt is more notable when the grain size is smaller (Figure 14).

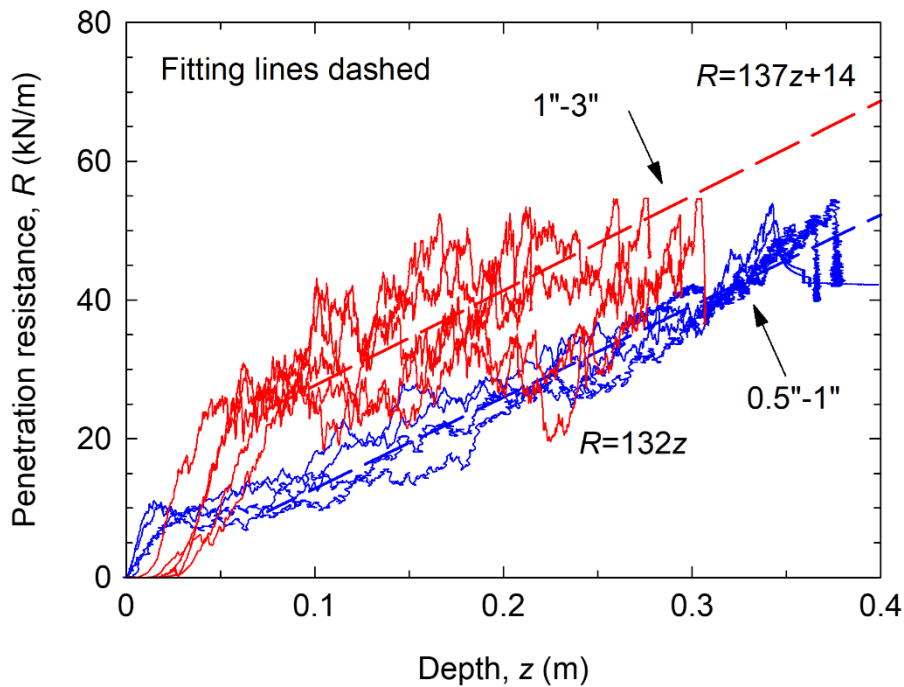


Figure 13. Penetration resistance of 15 mm-thick bevelled skirt in both gravels.

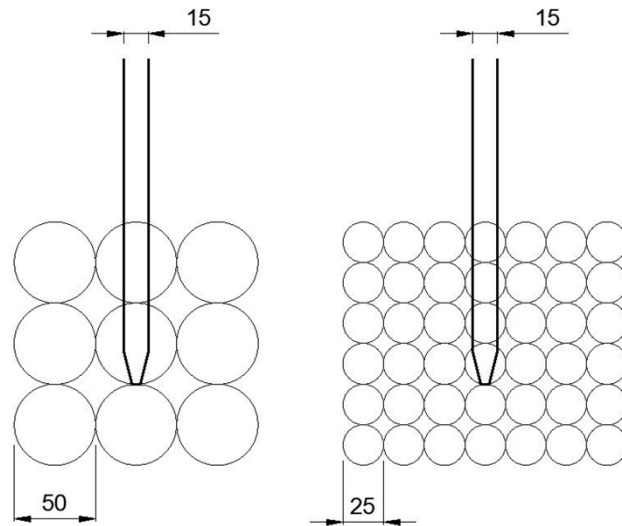


Figure 14. Representation of 15mm-thick bevelled skirt in both gravels (particles idealized as spheres with a uniform diameter of d_{50}) (units in mm).

Table 3. Reduction of vertical penetration force between flat tip and bevelled skirt for both gravels (experimental values obtained for a penetration depth of 200 mm).

	Flat Tip	Bevelled	Reduction %
$d_{50}=25$ mm	29.0 kN	26.4 kN	-9%
$d_{50}=50$ mm	44.6 kN	41.4 kN	-7%

4 NEW SEMI-EMPIRICAL APPROACH

Bearing capacity formulae or correlations based on cone penetration resistances are commonly used to study the penetration resistance. In the case of penetration in gravel, correlations with cone penetration resistances (e.g., DNVGL-RP-C212 2017) are not suitable because Cone Penetration Tests (CPT) are not appropriate in gravels. Consequently, empirically obtained correlation factors are only available for sands and clays. In the present section, a bearing capacity semi-empirical formula will be derived from the experimental data and also used to back-analyse the results from the tests.

Based on the interpretation of skirt penetration data from experimental tests in dense sands, Andersen et al. (2008) analysed different procedures to calculate penetration resistances, including bearing capacity formulae. The bearing capacity is composed of

two terms: (1) the tip resistance (R_{tip}) and (2) the side wall (shaft) resistance (R_{side}). They can be expressed as follow:

$$R = R_{tip} + R_{side} = q_{tip}A_{tip} + \int_{A_{side}} f_s dA \quad (1)$$

where A_{tip} is the tip area. Given a plane strain case, the tip area is directly the skirt thickness, (t). q_{tip} is the tip resistance, which is the key value in this case and is often obtained from experience. f_s is the side wall friction and A_{side} is the side wall area ($2 \cdot z$ in this case). Based on strength parameters obtained directly from laboratory tests (namely, the friction angle, ϕ , in this case of a purely frictional material), the tip resistance and the side wall friction can be expressed as follow:

$$q_{tip} = 0.5\gamma' t N_\gamma + q N_q \quad (2)$$

$$f_s = K\gamma' z \tan\delta \quad (3)$$

where γ' is the effective unit weight (submerged in this case) (here, an average value of $\gamma' = 12.3 \text{ kN/m}^3$ was used, Table 1), N_γ and N_q are the bearing capacity factors, which depend on ϕ , ($N_\gamma = 1.5(N_q - 1)\tan\phi$, $N_q = e^{\pi \tan\phi} \tan^2(45^\circ + \phi/2)$), q is the effective overburden pressure at the tip level ($q = \gamma' z$), δ is the friction angle between the gravel and the skirt walls (assumed in this case as $\delta = 0.9\phi$) and K is the coefficient of earth pressure (ratio between horizontal and vertical effective stresses). For the theoretical back-analysis of the experimental results, $K = 0.95$ was assumed as an intermediate value between the value of 0.8 recommended by the API RP 2GEO (2011) and the value of 1.1 recommended by Andersen et al. (2008). In any case, K and δ have a negligible influence on the results because they are involved only in the wall friction resistance (see Eq.3), which is less than 3% of the total penetration resistance for the cases analysed (Table 4). The tip and side penetration resistances in Table 4 were obtained using Eqs. 1-3 with a back-calculated friction angle as explained in the following.

Table 4. Tip and side penetration resistances (in kN) obtained from the back analysis of flat tip skirt penetration ($z=200$ mm).

R (kN)	$t = 15$ mm		$t = 80$ mm		$t_{eq} = 15 + d_{50}$ mm		$t_{eq} = 80 + d_{50}$ mm	
	R_{tip}	R_{side}	R_{tip}	R_{side}	R_{tip}	R_{side}	R_{tip}	R_{side}
d_{50}								
25 mm	28.4	0.53	--	--	27.9	0.45	--	--
50 mm	44.0	0.56	104.0	0.48	43.5	0.44	103.5	0.43

The key parameter that controls the penetration resistance is the gravel friction angle, which could not be measured in the laboratory due to the large grain size of the gravel. Thus, it was decided to back-calculate its value using Eqs. 1-3 based on the experimental results for a penetration depth of 0.2 m (which was the target penetration depth for this experimental campaign). Since the friction angle is expected to vary with the stress level, the back-calculated values may be assumed as average ones.

Table 5. Friction angle of both gravels obtained from the back analysis of flat tip skirt penetration ($z=200$ mm).

	$t = 15$ mm	$t = 80$ mm	$t_{eq} = 15 + d_{50}$ mm	$t_{eq} = 80 + d_{50}$ mm
$d_{50}=25$ mm	54°	--	49°	--
$d_{50}=50$ mm	56°	51°	48°	48°

The back-calculated values of the friction angle are summarized in Table 5 and show some disparities, namely $\phi=51^\circ$ for the 80 mm-thick skirt and 56° for the 15 mm-thick skirt in the 1"-3" gravel. These differences are mainly attributed to the grain size effect, i.e., the differences in the t/d_{50} ratios (0.3 vs. 1.6).

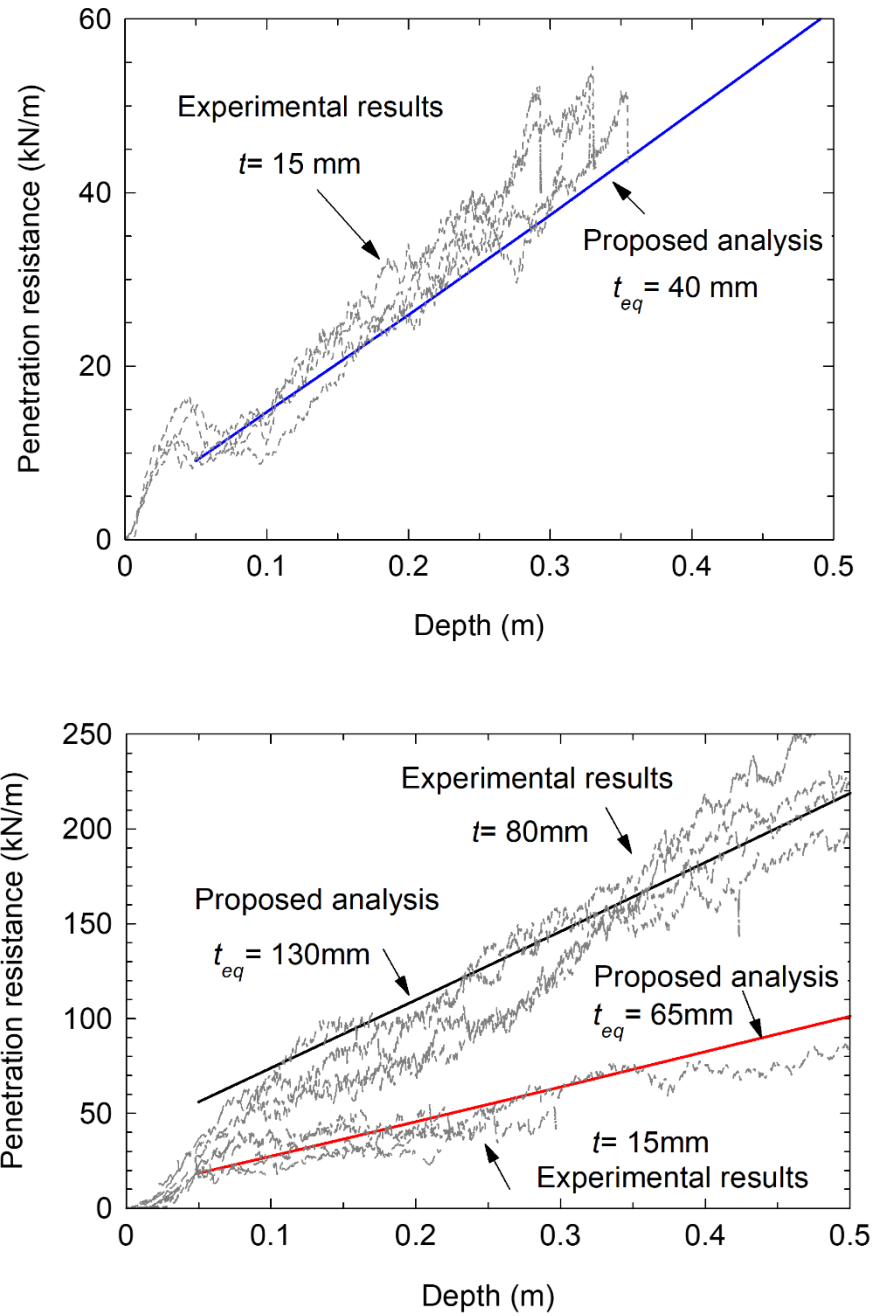


Figure 15. Back-analysis using the proposed approach (based on Andersen et al. 2008 and Miyai et al. 2019) of the experimental fittings from the tests with the 15 mm- and 80 mm-thick flat tip skirts: (a) 0.5"-1.5" gravel; (b) 1"-3" gravel.

To account for the grain size effect in the penetration, the experimental results were re-interpreted using not the real skirt thickness (t), but an equivalent thickness that is equal to the average grain size plus the real thickness of the skirt ($t_{eq} = t + d_{50}$), as proposed by Miyai et al. (2019). The back-calculated values of ϕ using this equivalent thickness

(see Table 5) are highly consistent as the same value ($\phi=48^\circ$) is found for the 1"-3" gravel for both skirt thicknesses and a slightly higher value ($\phi=49^\circ$) is obtained for the finer gravel (0.5"-1.5"). The theoretical predictions using t_{eq} and these back-calculated friction angles are compared with the linear fittings of the experimental results in Figure 15, showing a good agreement. Therefore, although all the back-calculated friction angles (Table 5) are within a possible range for these gravels (e.g., Moroto and Ishii, 1990; Indraratna et al. 1998; Varadarajan et al. 2003), the consistency of the values obtained using t_{eq} suggests that the hypothesis presented by Miyai et al. (2019) offers good results. The underlying physical phenomenon that justifies the use of an equivalent plate thickness is the fact that when the grain size is comparable to the plate thickness, some grains interlock with the plate tip and accompany it, enlarging the penetrating tip area (e.g., Miyai et al. 2019, Figure 14). For example, in the limit case of a comparably very thin plate ($t \approx 0$), the penetrating element could be assimilated to the thin plate with a grain (or a row of grains in three-dimensions) at the tip ($t_{eq} \approx d_{50}$), assuming the grains do not break.

5 CONCLUSIONS

Full-scale tests were performed to study the penetration resistance of steel plates (skirts) in gravel. Penetration resistance is well studied in clays and sands, but there is limited information on penetration in gravels, which are typically used in scour protection systems. This knowledge gap has been addressed by means of a set of real scale tests. Two steel plate thicknesses and two gravel sizes (providing t/d_{50} ratios between 0.3 and 1.6) were used to study the influence of the grain size effect, i.e., when the grain size is comparable to the skirt thickness.

The results of the experimental tests verify that the penetration resistance increases with the penetration depth, the skirt thickness and the gravel grain size. The penetration consisted of three main phases. A first phase where the resistance increases sharply at the beginning because the penetration mechanisms are not developed at all. Beyond a specific depth, the penetration resistance increases linearly with depth because the penetration mechanism (flow of the gravel grains to the sides of the tip) has been fully developed (third phase). Between these two phases, there is an intermediate (transient) one (second phase), where the load-displacement curves show a decrease and a plateau, associated with the triggering of the penetration mechanism.

The experimental measurements showed some irregularities (noise) in the penetration resistance law (particularly in the second and third penetration phases). These irregularities were found to be greater when the t/d_{50} ratio was smaller. Therefore, they can be linked to the grain size and the accommodation of the grains around the tip when the skirt penetrates in the soil.

Traditionally, bevelling the skirt tip is a proven strategy with lower grain sizes. However, in the case of gravel, this strategy provided a limited reduction of the penetration resistance of around 10% for the studied cases.

For the theoretical interpretation of the experimental results, satisfactory agreements were found when coupling traditional approximations like Andersen et al. (2008) with the equivalent skirt thickness hypothesis proposed by Miyai et al. (2019). Consequently, based on the results obtained, using this equivalent skirt thickness is the suggested calculation method. In future studies the current experimental data base will be expanded by combining a wider range of gravel sizes, skirt thicknesses and gravel types in order to increase the reliability of this approach for a wider range of combinations. Besides, additional factors, such as grain crushing and the interaction between closely-spaced penetrating elements should be considered.

DATA AVAILABILITY STATEMENT

All data, models, or code that support the findings of this study are available from the corresponding author upon reasonable request.

ACKNOWLEDGEMENTS

This research has been conducted by IHCantabria within the framework of the design process of DolWin kappa structure (DolWin6 Project). The authors would like to thank TenneT, DRAGADOS OFFSHORE and SIEMENS for their support of this research.

Raúl Guanche also acknowledges the financial support from the Ramon y Cajal Program (RYC-2017-23260) of the Spanish Ministry of Science and Innovation.

Elena Varela also acknowledges financial support from the Spanish Ministry of Economic Affairs and Digital Transformation (MINECO) and the European Regional Development Fund (ERDF) through the project “Foundation of offshore platforms for renewable energies” (PEJ2018-003335-A) with financial resources from the Youth Employment Initiative (YEI) and the European Social Fund (ESF).

REFERENCES

- Andersen, K.H., Jostad, H.P., Dyvik, R. 2008. Penetration resistance of offshore skirted foundations and anchors in dense sand. *Journal of Geotechnical and Geoenvironmental Engineering* 134, 106-116.
- API (American Petroleum Institute). 2011. Petroleum and natural gas industries—Specific requirements for offshore structures, Part 4—Geotechnical and foundation design considerations. API RP 2GEO.
- Bienen, B., Gaudin, C., Cassidy, M.J., Rausch, L., Purwana, O.A., Krisdani, H. 2012. Numerical modelling of a hybrid skirted foundation under combined loading. *Computers and Geotechnics* 45, 127-139.
- Bolton, M.D., Gui, M.W., Garnier, J., Corte, J.F., Bagge, G., Laue, J., Renzi, R. 1999. Centrifuge cone penetration tests in sand. *Geotechnique* 49, 543-552.
- DNVGL. 2017. Recommended Practice DNVGL-RP-C212. Offshore soil mechanics and geotechnical engineering.
- Escribano, D.E., Brennan, A.J. 2017. Stability of scour protection due to earthquake-induced liquefaction: Centrifuge modelling. *Coastal Engineering* 12, 50-58.
- Feng, X., Gourvenec, S. and Randolph, M.F. 2014. Optimal skirt spacing for subsea mudmats under loading in six degrees of freedom. *Applied Ocean Research* 48, 10-20.
- Houlsby, G.T., Byrne, B.W. 2005. Design procedures for installation of suction caissons in sand. *Proc. ICE – Geotechnical Engineering* 158, 135-144.
- Indraratna, B., Ionescu, D., Christie, H.D. 1998. Shear behaviour of railway ballast based on large-scale triaxial tests. *Journal of Geotechnical and Geoenvironmental Engineering* 124, 439-449.
- Lian, J., Chen, F., Wang, H. 2014. Laboratory tests on soil-skirt interaction and penetration resistance of suction caissons during installation in sand. *Ocean Engineering* 84, 1-13.
- Liu, J., Duan, N., Cui, L., Zhu, N. 2019. DEM investigation of installation responses of jacked open-ended piles. *Acta Geotechnica* 14, 1805-1819.
- Mana, D.S.K., Gourvenec, S., Martin, C.M. 2013. Critical skirt spacing for shallow foundations under general loading. *Journal of Geotechnical and Geoenvironmental Engineering* 139, 1554-1566.

- Martin, C.M., Dunne, H.P., Wallerand, R., Brown, N. 2015. Three-dimensional limit analysis of rectangular mudmat foundations. *Frontiers in Offshore Geotechnics III – Meyer (Ed.)*. Taylor and Francis group, London.
- Miyai, S., Kobayakawa, M., Tsuji, T., Tanaka, T. 2019. Influence of particle size on vertical plate penetration into dense cohesionless granular materials (large-scale DEM simulation using real particle size). *Granular Matter* 21, 1-21.
- Moroto, N., T. Ishii. 1990. Shear strength of unisized gravels under triaxial compression. *Soils and Foundations* 30, 23-32.
- Riazi, A., Türker, U. 2019. The drag coefficient and settling velocity of natural sediment particles. *Computational Particle Mechanics* 6, 427-437.
- Senders, M., Randolph, M.F. 2009. CPT-Based method for the installation of suction caissons in sand. *Journal of Geotechnical and Geoenvironmental Engineering* 135, 14-25.
- Sonneville, B., van Velzen, G., Wigaard, J. 2014. Design and optimization of scour protection for offshore wind platform DolWin beta. *Proc. Of the ASME 2014 33rd International Conference on Ocean, Offshore and Arctic Engineering OMAE 2014*. June 8-13, 2014, San Francisco, California, USA.
- Varadarajan, A., Sharma, K.G., Venkatachalam, K., Gupta, A.K. 2003. Testing and modelling two rockfill materials. *Journal of Geotechnical and Geoenvironmental Engineering* 129, 206– 218.
- Villalobos, F.A., Byrne, B.W., Houlsby, G.T. 2010. Model testing of suction caissons in clay subjected to vertical loading. *Applied Ocean Research* 32, 414-424.
- Wu, Y., Yang, Q., Li, D., Zhang, Y., Wang, T. 2021. Resistance of caisson tip with internal bevels for suction caissons penetrating into clay. *International Journal of Geomechanics* 21, 04021091.